THE AMERICAN SOCIETY OF MECHANICAL ENGINEERS
345 E. 47 St., New York, N.Y. 10017

85-IGT-65

Investigation of a Tip Clearance Cascade in a Water Analogy Rig

J. A. H. GRAHAM
Staff Aerodynamicist
Pratt and Whitney Canada Inc.
Longueuil, Quebec, Canada J4K 4X9

ABSTRACT

The tip clearance flow region of high pressure axial turbine blades for small gas turbine engines has been investigated in a water flow cascade. The blade model features variable clearance and variable endwall speeds. The cascade is scaled for Reynolds number and sized to give velocities suitable for visualization. Pressure profiles were measured on one blade, and correlated with the visualization. Unloading is found to be a major feature of the pressure field at both tip and midspan, and is intimately connected with scraping effects and the behavior of the clearance vortex. Some initial hot film velocity measurements are also presented.

1.0 INTRODUCTION

Tip clearance flows are an important source of turbine energy losses. Major efforts have been expended in investigating these flows from an experimental and theoretical point of view, partly at least with the idea of inventing modifications to blades or shrouds to reduce energy losses. Our own efforts have hitherto concentrated on cold flow rig tests[1], in which efficiency could be measured against changes in hardware configuration.

Indeed the bulk of the research effort in this field has consisted of efficiency measurements on engine hardware. This is virtually as true today as in 1954 when Rains[2] noted the fact in his paper on clearance flow visualization in a rotating compressor water rig. Theoretical work has ranged from the geometrical correlations of Ainley and Mathieson[3,4] and others, through the body of theory based on lifting line theory, due to Lakshiminarayana and Horlock[5,6,7] to detailed analysis of the clearance gap flow itself[8]. Detailed modelled experiments of the tip clearance flow have also appeared in the literature[9,10].

Our investigations were prompted by certain baffling aspects of the cold flow turbine rig work, and by initial work on a detailed clearance gap flow analysis at P&WC that showed physical insight was lacking in certain areas. In particular the question of unloading towards the blade tip, and its dependence on clearance, needed quantification. Related to this is the effect of the clearance vortex on the suction surface pressure field, on the flow field in general, and on energy losses. There was also the question of frictional forces on the clearance flow itself. Although there is evidence in the literature[9,10] that clearance flows at large but realistic clearances are substantially potential, there was still a need to investigate scraping and frictional effects, especially at tight clearances. Thus we decided to include relative motion of blade and endwall in the experimental design. We also desired that the experiments could extend to the design of blade tip and endwall devices to reduce clearance losses. Accordingly it was decided to press the then-new Water Flow Analogy Rig into service, using cascade models with water as the working substance, in order to take advantage of the relative ease of visualizing flows in water at low speed. At the same time it was decided to develop pressure and velocity measuring techniques to quantify the investigation.

The Water Flow Analogy rig had already been developed for investigating highly complex flows that are not amenable to purely analytical treatment. It was designed for Reynolds number modelling of gas flows on the scale of our own small gas-turbine engine parts and is intended both as a research tool and as a means for optimizing the design of hardware in which a fluid flow is of critical importance.

The first research job for the rig is the present investigation into the mechanics of tip leakage flow. It was decided that the working section should consist of transparent, quasi-two dimensional plexiglass cascades having four channels separated by three blades with variable tip clear-

Presented at the 1985 Beijing International Gas Turbine Symposium and Exposition
Beijing, People's Republic of China – September 1-7, 1985

ance. This cascade flow is analogous to the gas flow in the blade tip and outer shroud region in the engine. The wall of the test section which corresponds to the shroud in the engine, consists of a moving belt which simulates the relative motion of blade tip and shroud. Different cascades, corresponding to different blade designs, can be inserted in the test section, while the surface treatment of the belt can simulate various shroud liner geometries.

Investigations consist of visual observations on the blade tip and shroud region for blades of different tip profile; pressure measurements at tip and mid-section on one instrumented blade and mean velocity measurements with constant temperature anemometer using hot film probes. Experiments with each cascade are shaken down with a stationary endwall and a clearance gap typical of engine practice. Configurations are then varied to include a variety of clearance gaps and endwall speeds, including the speed that correctly models the engine gas velocity triangles and blade speed.

2.0 DESCRIPTION OF RIG

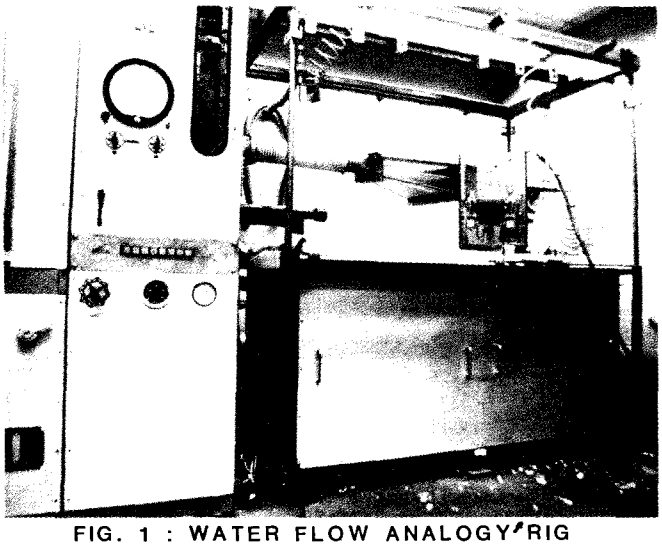

FIG. 1 : WATER FLOW ANALOGY RIG

2.1 General Description

The water rig (Fig 1) consists of a recirculating water system. Water is pumped from a storage tank (lower right) into a header tank (upper left) from which it runs through the test section (upper right) and returns to the storage tank. The photograph shows a blade cascade installed in the working area. In practice a wide variety of internal flow model or open water tables can be installed. Two pumps provide a maximum water flow of 260 gallons/min. delivered at the top of the auxiliary tank. A maximum head of 20 ft. is available. All parts of the system in contact with water are made of plastic, fibreglass or stainless steel, to avoid corrosion. The pumps are designed for slurry and can easily cope with polystyrene particles used for flow visualization.

A typical cascade (Fig. 2) consists of five plexiglas blades, each 6.5 inches long, having throughout their length a cross section modelled on a blade tip cross section. The blades are suspended vertically, with the simulated tip clearance at the floor of the cascade. The cascade duct, and the blades, are made of transparent plexiglas. Flush with the cascade floor, beneath the blades, runs the smooth rubber belt which simulates blade-shroud relative motion. This is stretched between pulleys which are driven by a compressed air motor with widely variable speed. The duct is operated full of water so that the flow in the blade channels has solid borders, and the secondary flows are in the correct direction. The scale of the model is eight times prototype, at the tip section. With full flow this gives a reasonable simulation of the engine Reynolds number, about 1×10^5, thus ensuring that dynamic effects are modelled. Compressibility effects are not modelled. This, with the partial two dimensional nature of the model arrangement, is the main shortcoming of the model.

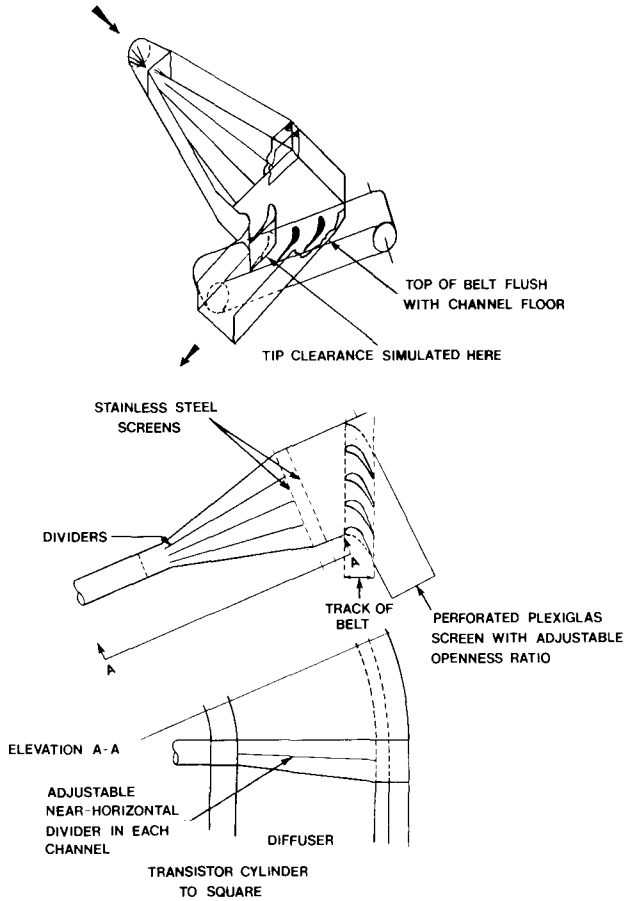

FIG. 2 : TIP CLEARANCE MODEL

2.2 Observations and Measurements

2.2.1 Flow Visualization

Two principal observation techniques were used. Firstly, the flow was seeded with neutrally buoyant polystyrene balls, which were selectively illuminated with a planar beam of light in different directions. The planar beam of light was produced by a mercury vapour lamp, enclosed in a metal reflector box from which the ozone produced by the light was withdrawn to outdoors by an extractor fan. This airstream was designed also

to cool the 1.0 kilowatt lamp. The light that leaves the box passes through collimating slits and a cylindrical lens, thus creating a near parallel (but focussing) beam of light for up to 12 or 24 inches from the lens.

Secondly, details of the flow were highlighted with dye streaks, delivered to desired points in the flow by easily positioned flexible hypodermic tubing. Tufts of wool were also, at times, taped to wall surfaces.

2.2.2 Pressure Measurements

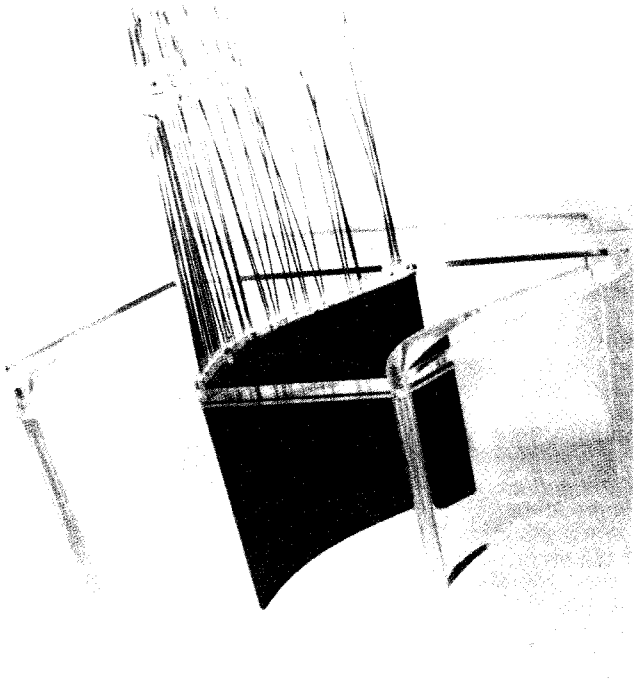

FIG. 3 : CASCADE WITH INSTRUMENTED BLADE

One of the blades (our R15) was instrumented with pressure tappings (Fig. 3) Ten tappings were made on each surface at both mid span, and at 0.125 inches from the tip. The pressure tubes are made of hypodermic, moulded into a blade made of Devcon, for which one of the plexiglas blades was master. The blade is carefully lacquered so that the tapping holes are correctly shaped. The 40 pressure lines are then connected, via swagelock connections and 1/16" dia. nylon flexible tubing, to a 48 Channel Scanivalve system. 8 channels, used for checking, are spread among the other 40. A very sensitive transducer is necessary to measure the pressure differences generated by a water flow of only 1 to 2 ft/sec. A Druck PDCR22 was chosen. It is completely compatible with water.

All the tubing is kept full of Merriam fluid, completely bubble free, during measurements. This acts as a surfactant which prevents air bubbles from attaching themselves to tubing walls. The bleeding process is difficult and tedious. Much development time was spent in refining the system to make bleeding effective. Thicker, and opaque tubing was discarded, and a system was arrived at having constant tube cross section, and loose enough to allow bubble-hunting through the system. It was found necessary to replace the fluid in the system about every two months in order to clear coagulants that form in Merriam fluid, imparting to the measuring system a most unwelcome hysteresis. There is a Merriam-fluid: water interface at the pressure tappings or in the tubing nearby when the system is running. Merriam escape into the general water system must be limited because its excessive presence causes air entrainment and bubbling, which prevents accurate pressure measurements, and is detrimental to hot film velocimetry.

2.2.3 Hot Film Anemometry

A simple system of hot film anemometry was developed for mean velocity measurements in the cascade channels and in the clearance gap. The bridge anemometer is a DISA 56C01 (multichannel) rack system constant temperature anemometer with a 56N221 mean value unit, consisting of DVM, integrator and filter. Signals are not linearised. Instead, calibration curves are set up by running the CTA in the calibration system described later. At the low velocities prevalent in our rig the calibration curves diverge somewhat from King's Law, and thus the normal lineariser, which assumes that King's Law is in operation, cannot be used. It is, in any case, unnecessary when analog measurement of turbulent quantities is not being performed.

3.0 FLOW VISUALIZATION

3.1 General

Two radically different types of tip section were investigated: two examples of the first, fairly thick blade (t/c = .175) and one of a 'squealer' tip (t/c = .042). One of the thick blades was instrumented for pressure measurements, as will be reported later on. These radically different blade sections are considered to represent extremes in the range of possible shapes in tip sections, at least for our small gas turbine high pressure blades.

In order to model Reynolds number (about 10^5, based on chord) the flow is run between 80 and 240 gpm, with an 8:1 enlargement of scale to keep velocities low enough for visualization. The test section is arranged with outer shroud and clearance gap at the floor, and the cascade suspended inside the duct. Thus the gravity induced pressure distribution in the water model is in the same direction as the centrifugally induced pressure gradient in the engine, and is close to the right magnitude. As the model flow is incompressible, Re simulation cannot extend to all parts of the flow field; but a reasonably close approximation can be achieved.

3.2 Observations

With water flux set to simulate Re, the endwall was run at various speeds: stationary, for preliminary shakedown and to establish a 'standard'

case; the correct speed for engine velocity triangle simulation (EES), and also one faster speed, about double EES, and a slower one, about half EES.

3.2.1 Thick Tipped Blade

Figure 4 shows the suction surface flow, and Figure 5 the flows viewed in planes crossing the blade to blade channel. Endwall is stationary in each case. The short markings show local flow vectors, while the long arrowed lines are typical streamlines. The heavy broken line marks the vortex boundary.

The secondary flow is well developed in Figure 4 and can be seen as a convergence in the flow direction along the suction surface at hub and tip. The vortex caused by the efflux of clearance gap flow into the channel is quite obvious near the tip of the blade, towards the trailing edge. The vortex begins about one third of the way along the curve of the suction surface. The cross sectional views (Fig. 5) show this vortex, with the secondary vortices, as they develop downstream. There is no vortex in the leading part of the suction surface, as a threshold strength appears to be necessary for the overshoot and rolling up process necessary to form it.

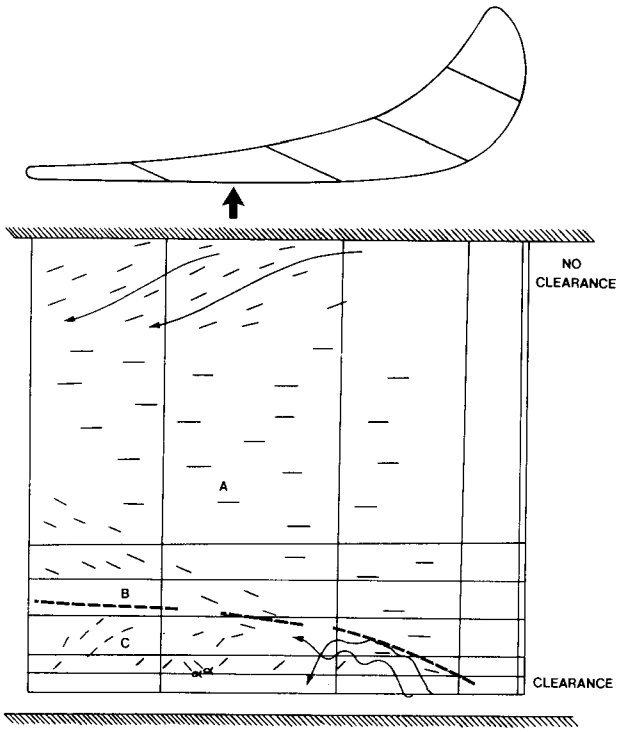

FIG. 4 : SUCTION SURFACE FLOW DISTRIBUTION WITH CLEARANCE OF 2.5% AT ZERO BELT SPEED

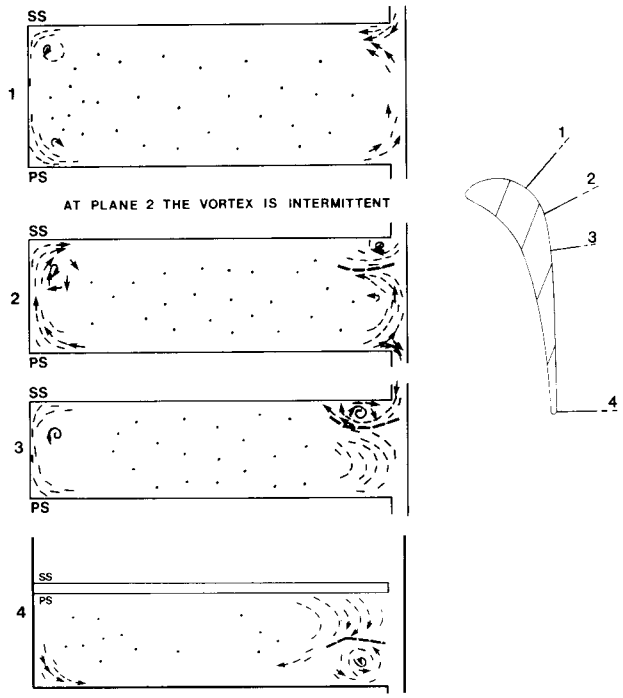

FIG. 5 : SECONDARY FLOWS IN CHANNEL BETWEEN BLADES WITH CLEARANCE OF 2.5% AT ZERO SPEED

3.2.1.1 Variation of Clearance

Figures 6 & 7 form a digest of plan views of flow in the clearance gap at a variety of clearances up to 2.5% of equivalent blade span, which is the span that a three dimensional model of the entire blade at 8:1 scale would have. This clearance equals 3.85% of the cascade blade span, and 3.45% of blade true chord at the tip. Clearance is given in terms of equivalent span throughout the paper. Speeds of endwall vary also. If we look through figures 6 & 7 we see that at zero endwall speed leakage flow tends towards the normal to the pressure surface, as clearance is reduced. Viscous domination of the flow increases, and the influence of the entry velocity to the gap reduces.

With the endwall in motion, leakage flow is reduced as clearance is reduced, and the belt boundary layer occupies a relatively increasing proportion of the gap space. The pressure driven clearance flow is turned towards the (engine) axis and is eventually drawn almost parallel to the direction of the moving belt. At this separation (0.6%) there is no leakage flow. At 1.2% there is some leakage flow, but its vortex is very weak. At greater belt speeds vortex behavior is qualitatively similar, but equivalent phenomena occur at greater separation. At higher speed there is also more mixing between the two flow regions in the clearance space. Turbulence is more energetic. The reduction of clearance flow (at any belt speed) is non linear, and no simple formulation is likely.

At engine equivalent speed (EES) the vortex onset position moves downstream as clearance is reduced and disappears between 1.2% and 0.6% clearance. At these clearances, there is a region of reduced clearance flow in the trailing edge region. This

increases in size as clearance is reduced. With belt at EES, and a clearance of 0.6%, there is no pressure driven clearance flow at all.

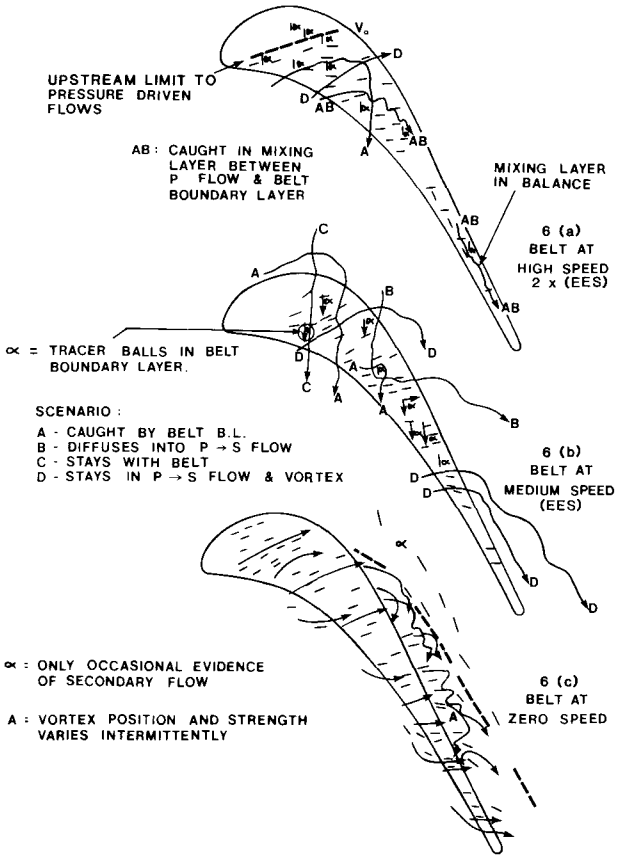

FIG. 6 : TIP CLEARANCE FLOW COMPARISON WITH MAXIMUM CLEARANCE OF 2.5% AT VARIOUS SPEEDS

3.2.1.2 Speed Variation

In the clearance gap we have observed, as outlined above, that the pressure driven clearance flow and the endwall boundary layer act in opposition when the endwall is moving. At any given clearance increasing the belt speed reduces the clearance flow quantity, and at tight clearances (1.2% or 0.6%) leakage flow can be cut off by increasing the belt speed.

3.2.2 Implications

At tight clearances, increasing the speed has roughly the same effect as reducing tip clearance. It reduces or cuts out the leakage flow, by changing its direction and reducing the leakage layer thickness. This has implications in the desirable velocity triangle design at the tip section of a blade. It confirms the notion that reducing loading at the tip will reduce clearance losses, by making use of the endwall scraping effect. We return to this point in s4.3, after discussing the pressure measurements.

For purposes of leakage loss control, it appears that leakage reduction devices are needed only in the central part of the blade section, at least for the wide section type of blade we have here.

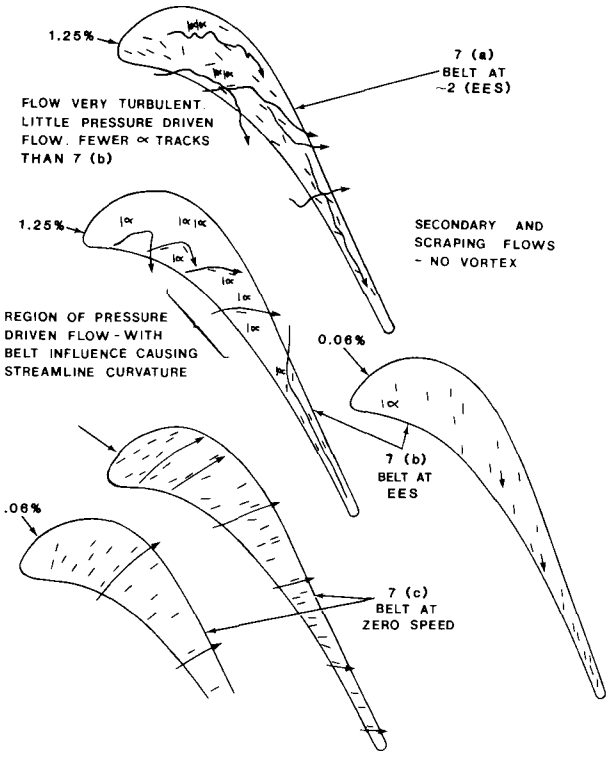

FIG. 7 : TIP CLEARANCE FLOW COMPARISON WITH CLEARANCE OF 1.25% AND 0.6% AT VARIOUS SPEEDS

Efforts should probably be focussed on annulling the leakage vortex, for several reasons. The leakage vortex can cause separated flow on the suction surface near the tip, while its enhancement of pressure loading at the tip section increases leakage flow. It disrupts channel flow and delivers off-design flow to downstream engine stages. Leakage flows too weak to form a vortex would appear to cause disproportionately reduced losses.

3.2.2 Thin Tipped Blade

Similar observations were performed on a thin tipped blade cascade representing a PT6 high pressure turbine blade tip section. The model blades were formed of curved plexiglas sheet of uniform thickness, with correctly rounded leading and trailing edges. Belt speed and clearance were varied as with the thick tipped blade.

Figures 8 & 9 show the passage vortices schematically, and define the clearance lines for the thin blade. The broad patterns of channel flow resemble those outlined above; there are however marked differences in the tip leakage region. As Figures 8 to 11 show, the blade tip is so thin that the leakage flow passes directly, in virtually straight lines, normal to the pressure surface. The short trajectory of pressure driven flow in the clearance gap means that it is hardly influenced by the tip and endwall boundary effects, except very close to these boundaries.

3.2.2.1 With the Moving Belt

The thin blade design is a compromise design in which the contours are quite a departure from

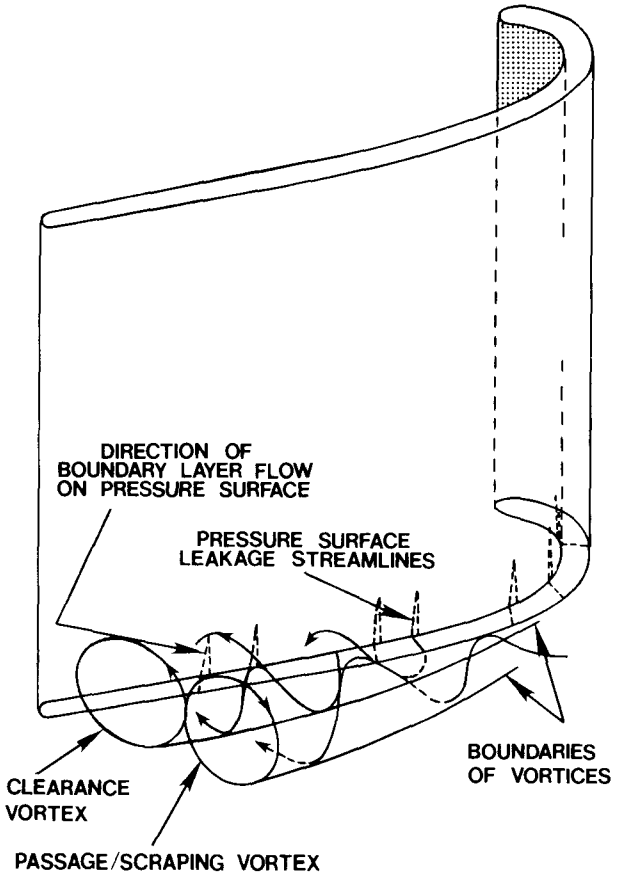

FIG. 8 : CLEARANCE AND PASSAGE VORTICES

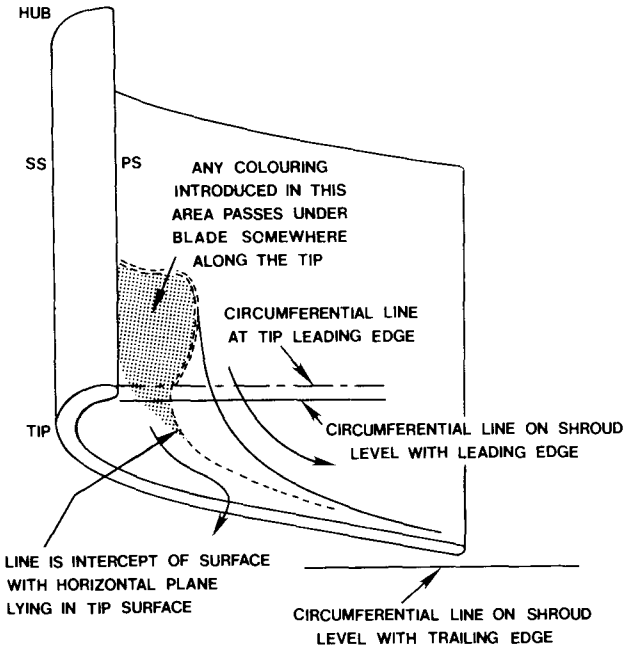

FIG. 9 : LEAKAGE LINE ON PT6 BLADE

channel design requirements. The channel flow is expected to be less than ideal; and the cascade flow shows this in Figure 10. Near the pressure surface, in the deeply concave section, there is stagnant flow on the verge of separation. Surface flow descends almost vertically (that is, almost radially outward in the engine situation) before entering the clearance gap. Mid stream flow markers confirm the existence of the stagnation region.

Rolled up secondary flow vortices are made strikingly visible by the dye streak technique in this channel. These intermittently roll up and the vortex line stretching as the flow leaves the stagnation region produces exceptionally rapid, tightly rotating flow.

The straight, near normal to pressure surface, tip gap flows retain these characteristics from the leading edge for about 60% of the blade chord. After that there is a slowly increasing divergence from the normal towards the trailing edge, reaching perhaps 30° or 40°. These flow angles remain the same at all tip clearances, for both stationary and moving belts. Thus the pressure difference between the blade surface overwhelms all surface frictional effects, in the clearance range used here, for the main clearance flow. At the smallest clearance, 0.6%, the pressure driven clearance flow is reduced. The leakage lines in Figs. 10 & 11 show how leakage flow is reduced as clearance is reduced. Pressure driven clearance flow direction is not affected.

The foregoing suggests that the thin tipped blade will be unresponsive to schemes that seek to reduce leakage flow by introducing additional drag to the clearance gap walls. This has already been observed in cold flow turbine rig efficiency measurements.

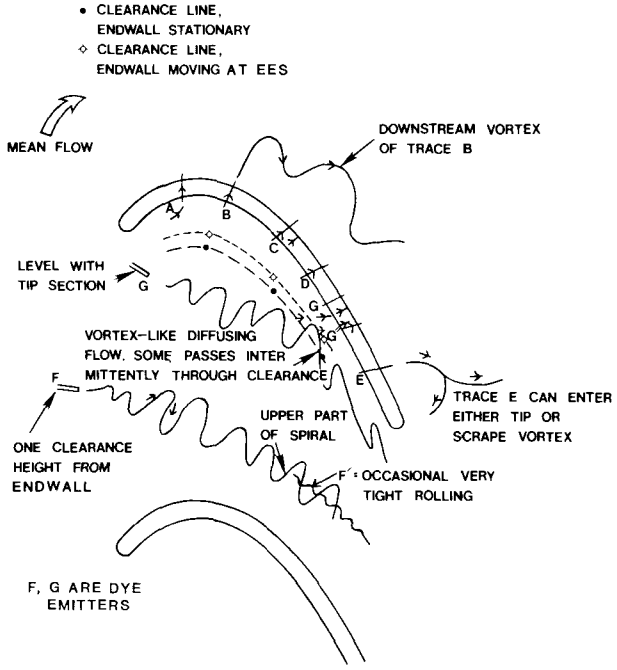

FIG.10 : CLEARANCE GAP FLOWS FOR MOVING ENDWALL, GAP 2.5% SPAN

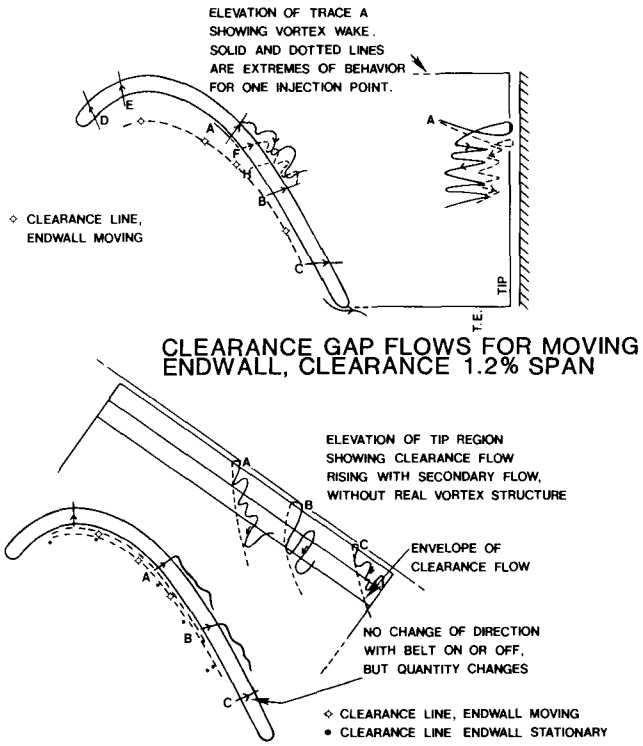

FIGURE 11

4.0 PRESSURE MEASUREMENTS ON THE INSTRUMENTED BLADE

A thick R15 blade was instrumented with pressure tappings on both pressure and suction surfaces at blade tip and midspan. These 40 tappings are connected through the tubing system to the scanivalve and pressure transducer outlined in s 2.2.2. After a lengthy shakedown period excellent reproducibility of data was achieved. With air rigorously excluded from the system the scatter of any single piece of data is very close to Gaussian and dependable results can be obtained by averaging over a sufficiently large sample. While there is some damping of random pressure fluctuations in the approximately metre-long tubing, there is only a short integration time in the transducer-D.V.M. system. Averaging, then, is achieved by accumulating a large sample at each data point.

Data is taken sequentially, with the 40 pressure measuring points interspersed with 8 constant 'check' pressures. Thus any unexpected changes can be detected as they occur, and spoiled data edited out of the record. As many as 20 records at any given flow condition are collected, and some data points repeated at the end of an experiment to ensure there has been no drift.

As before, data is collected with the end wall stationary, at engine equivalent speed, and at a speed nearly twice this. Clearance gap is varied between zero and 2.5% of equivalent blade span. A selection of these pressure plots is presented in Figures 12 to 18. In each the ordinate is pressure, while the abscissa is position along the direction of the engine axis. Four pressure contours are depicted: one each at midspan and at the tip on the pressure and suction surfaces.

4.1 Endwall Stationary

Let us first consider the cases with stationary end wall. Fig. 12 has large clearance (2.5%). In the forward part of this blade the unloading is quite evident and appears to be as great as 50%. Perhaps surprising at first sight, the reversal of this unloading in the downstream part of the suction surface is attributable to the powerful vortex that sits off the suction surface at the tip. As the line of pressure tappings is imbedded in the vortex the pressure will be significantly lower than the channel flow alone would lead us to expect. Now consider Fig. (14). Here the clearance gap is 0.6% and the leakage flow, too weak to form a vortex, merely joins the secondary flow creeping up the suction surface away from the tip (Section s3.2.11, Figs. 6 & 7). The vortex pressure signature on the suction surface is virtually absent. In the the forward part of this blade unloading is reduced to about 25% to 30%, undoubtedly because of the severely restricted clearance flow. A view of Fig. 15 takes this one step further. Here there is no clearance gap, and the pressure surface profiles at tip and midspan are

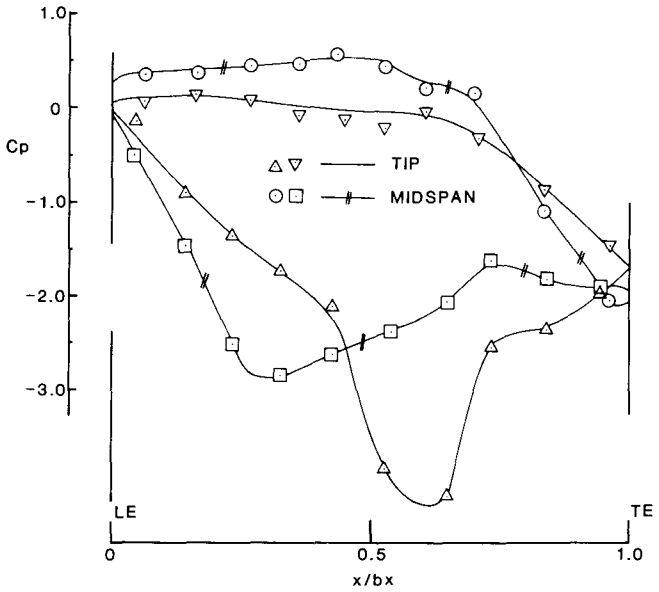

FIG. 12 : PRESSURE PROFILES AROUND BLADE CLEARANCE 2.5%, ENDWALL STATIONARY

virtually coincident. There is still unloading on the suction surface which is associated with the secondary flow. An intermediate case - Figure 13 - for 1.8% clearance is very similar to the 2½% clearance case, though milder both in its unloading in the forward part of the blade and in the pressure drop caused by the clearance vortex.

An examination of the midspan pressure curves in Figures 12 to 15 shows that unloading effects are apparent at midspan as clearance is increased. This is to be expected as midspan is less than half a blade chord from the tip.

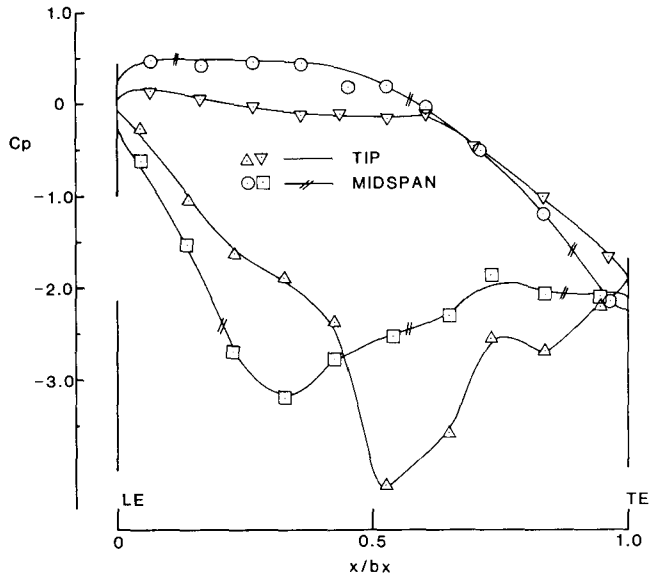

FIG. 13 : PRESSURE PROFILES.
CLEARANCE 1.8%, ENDWALL STATIONARY

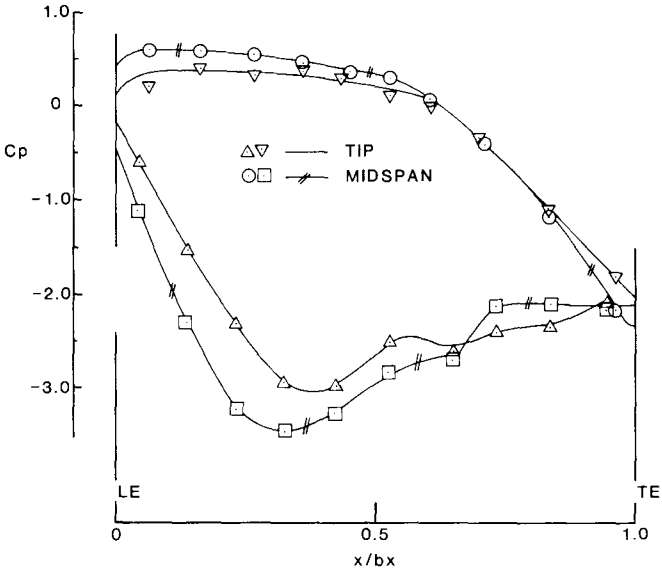

FIG. 14 : PRESSURE PROFILES.
CLEARANCE 0.6%, ENDWALL STATIONARY

4.2 Endwall in Motion

Movement of the endwall affects flow and pressure distributions most strongly at small separations (s 3.2.1.1). Thus in Figure 16, which shows the endwall at engine equivalent speed, at 2.5% separation, the pressure distribution and unloading are basically similar to Fig. 12, where endwall is stationary. There is however a significant reduction in the vortex strength, demonstrated by the reduced pressure effect at the tip, towards the trailing edge. Further increase of end wall speed, to nearly double engine equivalent, causes further, more striking change, as seen in Figure 17. Now the forward unloading is reduced greatly, and the vortex strength is reduced to vanishing. This corroborates the visualization work, reported above. The reduction in overall loading, which is stronger at the midspan section, is probably due to the high scraping effects and the circulatory

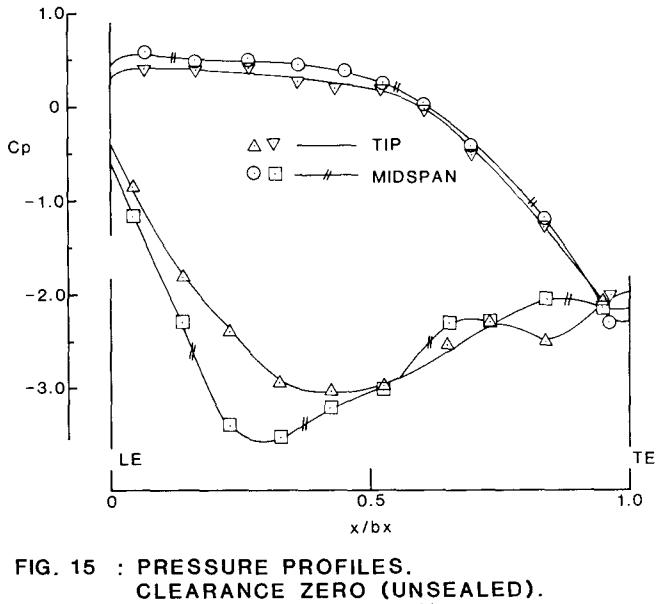

FIG. 15 : PRESSURE PROFILES.
CLEARANCE ZERO (UNSEALED).
ENDWALL STATIONARY

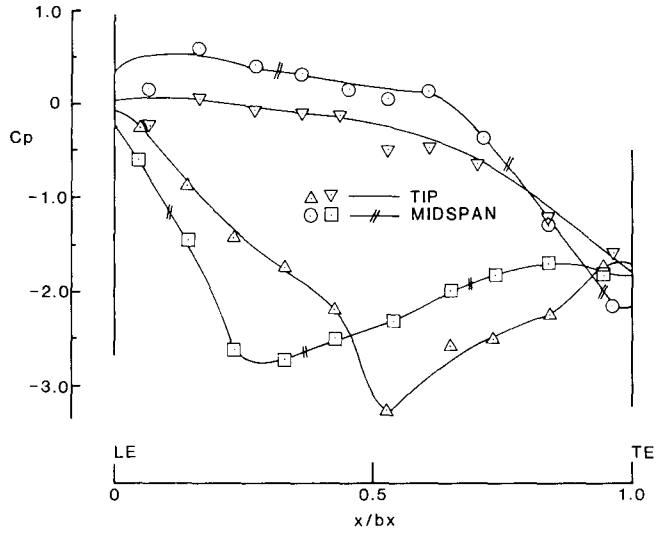

FIG. 16 : PRESSURE PROFILES.
CLEARANCE 2.5%, ENDWALL AT EES

channel motion that it causes.

Engine equivalent speed at 0.6% clearance is demonstrated in Figure 18. The difference to Fig. 14 is slight. Forward section unloading is reduced, and rear section unloading increased, at least on the suction surface. Visualization shows that at this separation, with endwall moving, there is no clearance flow at all. The secondary and scraping flows however tend to stagnate on the tip suction surface, thereby raising the pressure above the stationary wall case. A doubling of wall velocity causes significant change only in the suction surface tip pressures. These are raised to double or triple the differences at EES, due to the enhancement of the scraping effect.

4.3 A Summary of Clearance Flow Regimes

From the visualization work and the corroboration

provided by a pressure profile data a somewhat speculative plot of clearance vortex flow regimes has been prepared (Figure 19). Clearance and endwall speed are the variables. The boundaries between regimes of clearance vortex existence, and clearance flow without apparent vortex, are broad hatched regions to emphasize the fact that no sharp transitions of behavior are observed.

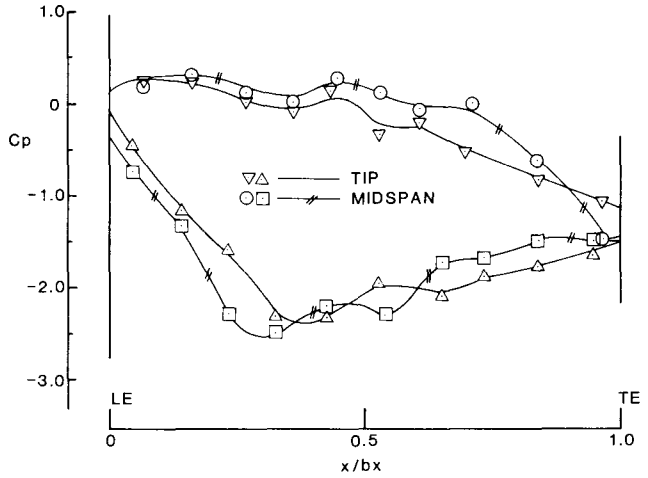

FIG. 17 : PRESSURE PROFILES.
CLEARANCE 2.5%, ENDWALL AT~2xEES

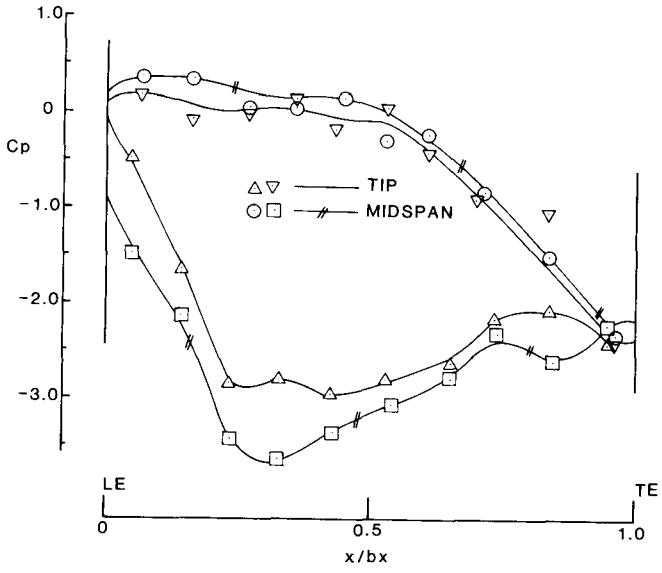

FIG. 18 : PRESSURE PROFILES.
CLEARANCE 0.6%, ENDWALL AT EES

4.4 Tip Loadng as a Function of Clearance and Endwall Speed

Figure 20 illustrates the dependence on clearance, of the ratio of tip loading to midspan loading at different endwall speeds. For stationary endwall this ratio is lowest for a clearance of about 0.6%, where the tip loading effect of the clearance vortex is absent. As the vortex builds up in strength at higher clearances, tip unloading is reduced near the trailing edge until tip and midspan loading are equal at 2.5% clearance. At engine equivalent speed, the curve follows the same trend, but with lower values of the ratio of loading because the vortex is weaker at any given clearance. At double engine equivalent speed the extreme tip unloading caused by scraping effects gives a very low value (0.42) for the loading ratio at a tight, 0.6% clearance.

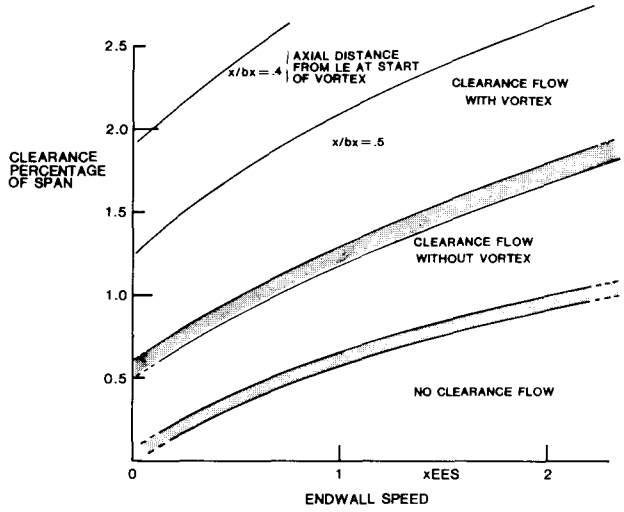

FIG. 19 : CLEARANCE VORTEX FLOW REGIMES

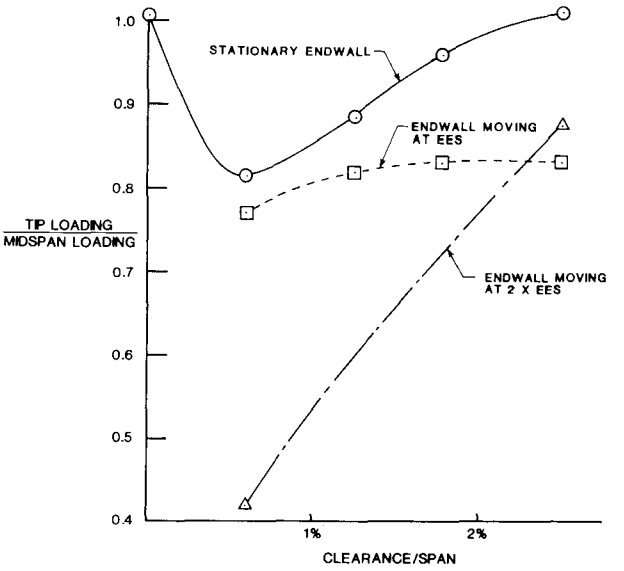

FIG. 20 : RATIO OF LOADING AT TIP TO MIDSPAN

5.0 VELOCITY MEASUREMENTS WITH HOT FILM ANEMOMETER

Velocity measurements have so far been restricted to the case of stationary endwall. Attention has been focussed on making velocity profiles in the blade to blade channel and in the clearance gap itself. Central to the question of measuring velocity is the question of flow direction and orientation of the probe. In a parallel homogeneous flow, if the probe is aligned with the flow, (that is, the sensitive element is normal to velocity direction) the anemometer registers maximum output voltage. Thus if the probe is oriented to give maximum output, we have found the flow direction. However, sensitivity to small deviations from flow direction is poor - far less than with a

cosine law - and our cascade flow is highly inhomogeneous. Thus we need the guidance of the visualization study to help setting up profile traverses. Though it is difficult to accurately determine direction with the anemometer probe alone, this does not adversely affect accuracy in the measurement of speed, because of the above mentioned insensitivity.

Calibration is carried out by running the probe and anemometer, with identical circuitry and overheat setting, in a small rig which consists of a 0.5 inch tube, 20.0 inches long, fed from the main test section, and discharging into a small rectangular reservoir with a weir. The probe is placed on the axis of the pipe at its exit into the reservoir. A turbulent velocity profile is assumed, as the pipe flow is turbulent over the range of operation, with a fine netting at its entry plane. The DISA anemometer is always set, for calibration and routine operation, at the same resistance, one that gives slightly more than 10% overheat for a water temperature of 70°F. The water temperature always rises slowly during operation - so a family of calibration curves was drawn up, each for a different water temperature. When operating, temperature is taken at the time each anemometer output is recorded. Frequent reference is made to standard velocity in the channel, to detect calibration drift from causes other than temperature change. Keeping the probe free of bubblesis sufficient to ensure calibration stability.

At the present time anemometry work has concentrated on clearance areas with stationary endwall. Figure 21 shows velocity profiles in the most active part of the clearance gap, close to the suction surface. Direction is as shown in the figure. At the greatest separation, there is a region of high velocity (U/U_O= 0.93 to 1.06, where U_O is average oncoming velocity.) in the lower half of the channel, and an extensive upper area moving more slowly (U/U_O = 0.25 to 0.65). This area is in the wake of the large entry bubble observed just inside the edge between the pressure surface and the tip surface. It is generally extensive enough at 2.5% separation to account for the size of this wake-like area. It should be noted that the channel flow in the clearance will be quite undeveloped, with very thin boundary layers on the bounding surfaces. These boundary layers are undoubtedly laminar, and in a typical fetch of 0.4 inch in the middle of the blade would have Re = 2,000, and δ^*, based on a laminar profile, of about 0.01 inch. The probe cannot reach this close to the wall because of its wedge shaped substrate, so the boundary layer of the clearance flow cannot be detected with the present equipment.

As the clearance gap is reduced to 1.9% from 2.5%, the extent of the bubble-wake region is significantly reduced, from 1.0% to 0.5% of equivalent span, with little change to the speed or extent of the main potential flow region. At 1.2% separation the wake region is much reduced in extent, and the main region slightly reduced in speed.

A vertical profile in the blade-to-blade channel, in Figure 22, gives a rather intriguing profile. In the two dimensional cascade one might at first sight expect a constant velocity, near the floor,

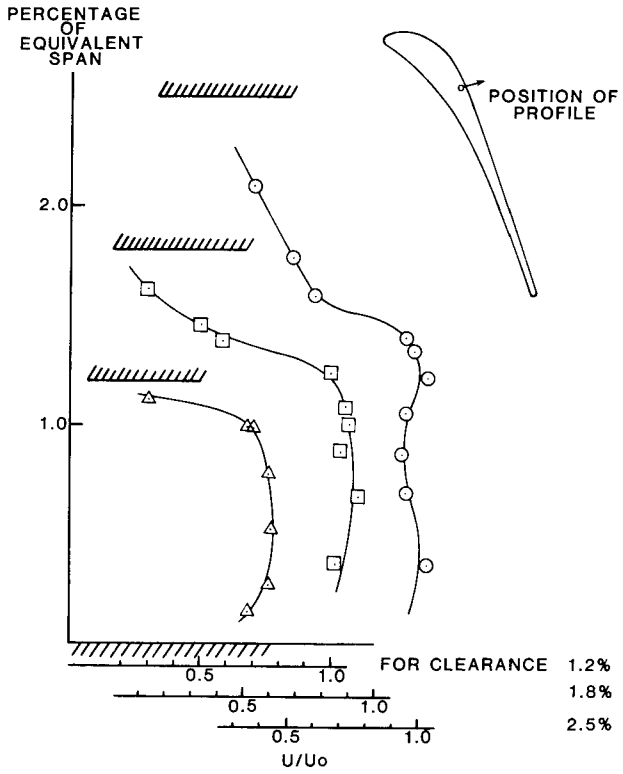

FIG. 21 : VELOCITY IN CLEARANCE GAP

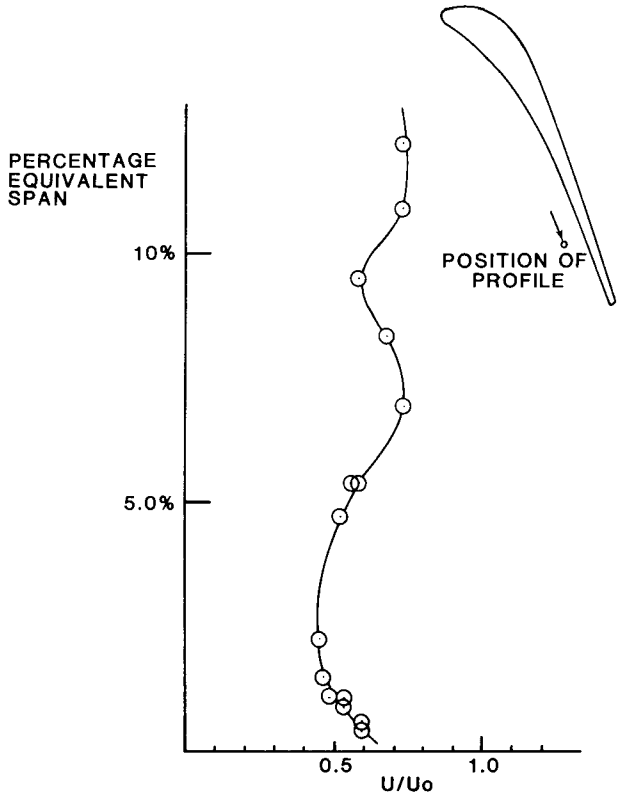

FIG. 22 : CHANNEL VELOCITY NEAR PRESSURE SURFACE

however, there is a marked reduction in velocity as the secondary flow sweeps the slow moving pressure surface flow into the position of the probe. This effect apparently abates before the wall boundary layer is felt.

6.0 CONCLUSIONS

Water model cascade tests have yielded, so far, much physical insight into tip clearance physics. Measurements of pressure and velocity in these same flows, at first doubtful because of the low water velocities, have proved successful, and capable of yielding detailed information about flow quantities, even in small scale regions of the flow.

It is clear that unloading is a major feature of the pressure field at both tip and midspan and is strongly dependent on the clearance, especially when reduced below 1.5% span. The clearance vortex, because of its deleterious influence on the channel flow and on downstream engine stages, appears to be a major cause of clearance losses, at clearances greater than about 1.25% span.

We are now at the point of being able to correlate clearance flux with pressure loading and clearance height. This will have a major impact on our detailed clearance gap analysis.

The visualization work especially shows that tip or shroud treatments intended to reduce clearance losses for any given clearance gap height can be localized in the central region of the blade. If such a device is just adequate to annul the clearance vortex, without removing the clearance flow completely, the best trade off between weight and/or complexity of the device, and efficiency improvement, will probably have been obtained.

Such efficiency improvement is most likely to be obtained on rather thick blades - indicating that minishrouds (winglets) may be desirable, especially for thin blades.

Progress to date indicates that further research should be directed towards blades with minishrouds, recessed tips, and towards various types of shroud treatment.

ACKNOWLEDGEMENTS

It is a pleasure to acknowledge the guidance of Mr. Ulo Okapuu, who instigated tip clearance research and the application of water analogy experimentation to turbine technology at P&WC. Some of the flow observations were made by Nader Pezeshkzad, who developed the ink streak visualization system.

REFERENCES

(1) Patel, K.V., "Research on a High Work Axial Gas Generator Turbine", S.A.E. Paper No. 800681, 1980.

(2) Rains, D.A., "Tip Clearance Flows in Axial Flow Compressor and Pumps", Cal. Inst. Tech. Rept. 5, June 1954.

(3) Ainley, D.G. & Mathieson, G.C.R., "An Examination of the Flow and Pressure Losses in Blade Rows of Axial Flow Turbines", R&M 2891, March 1951.

(4) Ainley, D.G. & Mathieson, G.C.R., "A Method of Performance Estimation for Axial Flow Turbines", R&M 2974, December 1951.

(5) Lakshminarayana, B. & Horlock, J.H., "Leakage and Secondary Flows in Compressor Cascades", Min. Tech. R&M 3483 (1965).

(6) Lakshminarayana, B. & Horlock, J.H., "Tip Clearance Flow and Losses for an Isolated Compressor Blade", Min. Tech. R&M 3316.

(7) Lakshminarayana, B., "Methods of Predicting the Tip Clearance Effects in Axial Flow Turbomachinery", ASME J. Basic Engineering, Vol. 92, 1970.

(8) Wadia, A.R., "Numerical Calculations of Time Dependent Three-Dimensional Viscous Flows in a Blade Passage with Tip Clearance", AIAA Paper No. 83-1171.

(9) Booth, T.C., Dodge, P.R., and Hepworth, H.K., "Rotor Tip Leakage: Part 1 - Basic Methodology", ASME Paper 81-GT-71, Gas Turbine Conference, March 1981.

(10) Wadia, A.R. and Booth, T.C., "Rotor Tip Leakage: Part II - Design Optimization through Viscous Analysis and Experiment", ASME Paper 81-GT-72, Gas Turbine Conference, March 1981.